Electronic Supplementary Information

A bifunctional robust metal sulfide with highly selective capture of Pb^{2+} ions and luminescence sensing ability for heavy metals in aqueous media

Anastasia D. Pournara,[a] Christina- Georgia Bika,[a] Xitong Chen,[d] Theodore Lazarides,[b] Spyridon Kaziannis,[c] Pingyun Feng,[d] Manolis J Manos*[,a,e]

[a]*Laboratory of Inorganic Chemistry, Department of Chemistry, University of Ioannina, 45110 Ioannina, Greece.*

[b]*Laboratory of Inorganic Chemistry, Department of Chemistry, Aristotle University of Thessaloniki, 54124 Thessaloniki, Greece.*

[c]*Department of Physics, University of Ioannina, 45110 Ioannina, Greece.*

[d]*Department of Chemistry, University of California, Riverside, CA 92521, USA.*

[e]*Institute of Materials Science and Computing, University Research Center of Ioannina, Ioannina, 45110, Greece.*

Email: emanos@uoi.gr

Details of the experimental setup and experimental procedure:

The laser induced fluorescence (*LIF*) experiments were performed at the *Central Laser Facility* of University of Ioannina, Greece using a custom-made experimental setup. The second harmonic (*SH*) of the output of an ultrafast *Ti:Sapphire* laser system is produced in a relatively thick *KDP* non-linear crystal and used as an excitation beam for **p-UCR-20** water solutions as a function of added micro-traces of heavy metal ions (Pb^{2+}, Cd^{2+} and Ni^{2+}). The spectrally compressed [1] *SH* pulses are set at 380 nm, which is well within the absorption of **p-UCR-20** sample. Moreover, they are temporally broadened to a sub-picosecond duration and only a small part of the *SH* beam (~ 5-7 μJ/pulse) is loosely focused (~ 6mm diameter) on the sample, reducing in that way the excitation intensity to avoid nonlinear absorption phenomena and thermal degradation. The pulse duration was measured using a home-made optical Kerr gate setup. A rough sketch of the experimental setup is shown below (Fig. S1) The sample is placed in a 1×1×5 cm quartz cuvette and it is diluted to a final concentration, which corresponds to an optical density of ~ 0.1 at 380 nm. The sample

is continuously refreshed using a magnetic stirrer and this is particularly important for the stability of the recorded *LIF* signal over time. The signal is collected through a long pass filter (cut off at 430 nm) at a 90° geometry, while at the same time a small part of the excitation beam is also measured and serves as a "*reference signal*" used to account for energy per pulse instabilities. The spectra of both signals are measured with a *UV-Vis* spectrograph consisting of an *Andor-Shamrock 303i* monochromator and *Andor iStar - CCD*. A *150 l/mm* grating was used to record simultaneously a region of 150nm of *UV-Vis* spectrum with *~1nm* spectral resolution. Exploiting the gated amplification of the CCD detector, fluorescence time "slices" as short as *1.5ns* can be recorded as a function of the time delay between the gate and the arrival time of the excitation pulse on the sample. The delay time is controlled with sub-nanosecond accuracy via a time-delay-generator (*Stanford Research Instruments*), "clocked" to the output of the *fsec* laser. The *CCD*-gate and therefore the temporal resolution of the *LIF* measurement is either set at *1.5 nsec* for fluorescent lifetime measurements or at *~50 nsec* for quasi steady state measurements. In the first case, the fluorescence lifetime is recorded as a function of heavy metal ions concentration. It is found that the integrated *LIF* signal follows a single exponential decay with a time constant of *4.0±0.2 nsec*, independently of the ion species or their concentration, suggesting that the quenching mechanism is predominantly of static nature. On the other hand, the *50 nsec* gate is long enough to collect the total *LIF* signal per pulse and typically several hundreds of single shot spectra are accumulated. The accumulation process is set for optimum detection sensitivity of heavy metal ionic micro traces in **p-UCR-20** water solutions, which is quantified indirectly by measuring the ratio of the *LIF* signal intensity to the excitation "*reference signal*" one. For each experimental run it is important to quantify the stability of this ratio and the associated error. Therefore, an hour-long data collection is taking place at first for heavy metal free **p-UCR-20** water solutions. The data are used to calculate the mean value of the ratio and its standard deviation, which is typically found to be 0.8 to 1.1 %. Each experimental run consists of a series of fluorescence intensity measurements as a function of the heavy metal ion added quantity. For each addition, a minimum of 20 minutes time interval is allowed for the sorption chemical process to be concluded. Following this procedure, the detection of micro traces (ppb levels) of Pb^{2+}, Cd^{2+} and Ni^{2+} ions is verified in water.

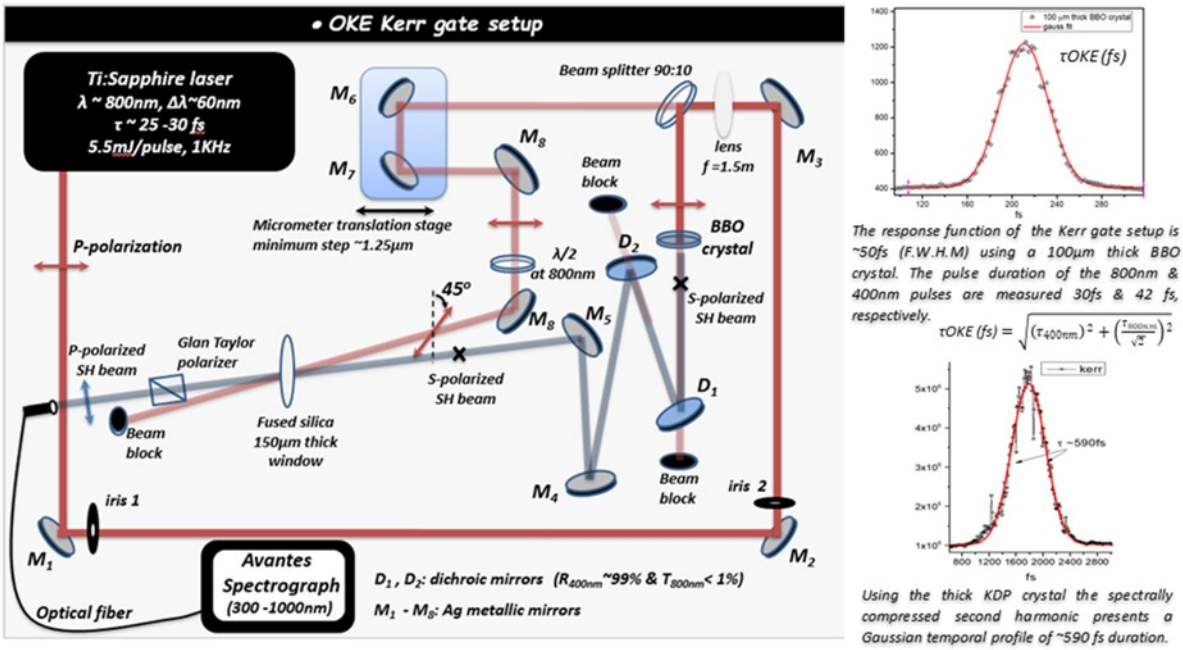

Fig. S1. Schematic representation of the experimental setup.

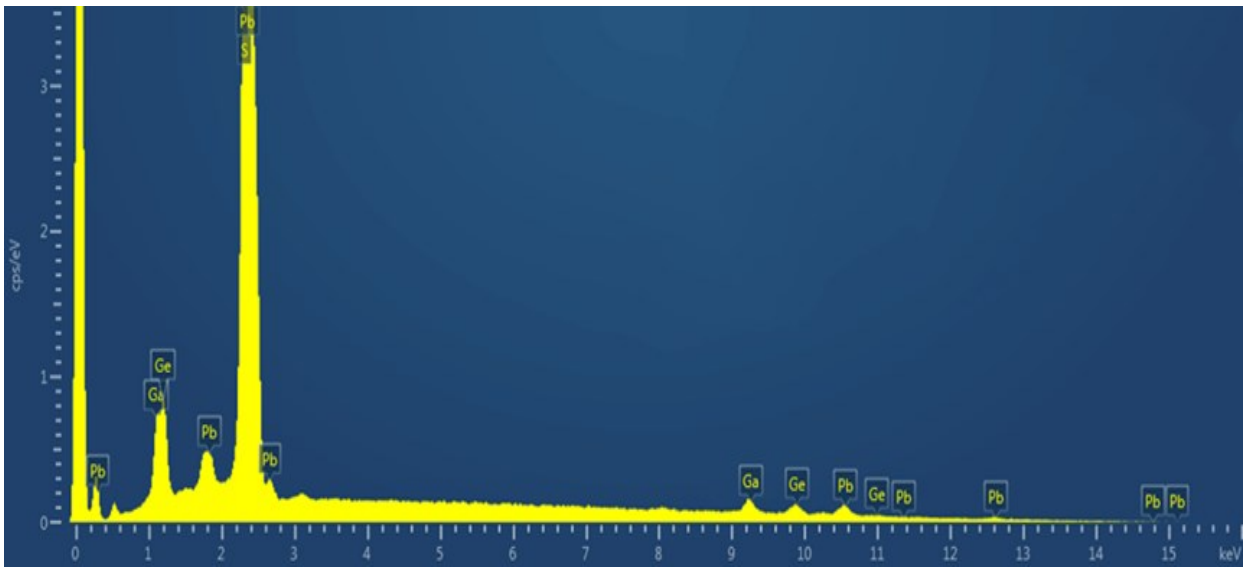

Fig. S2. EDS graph of Pb^{2+}-loaded material.

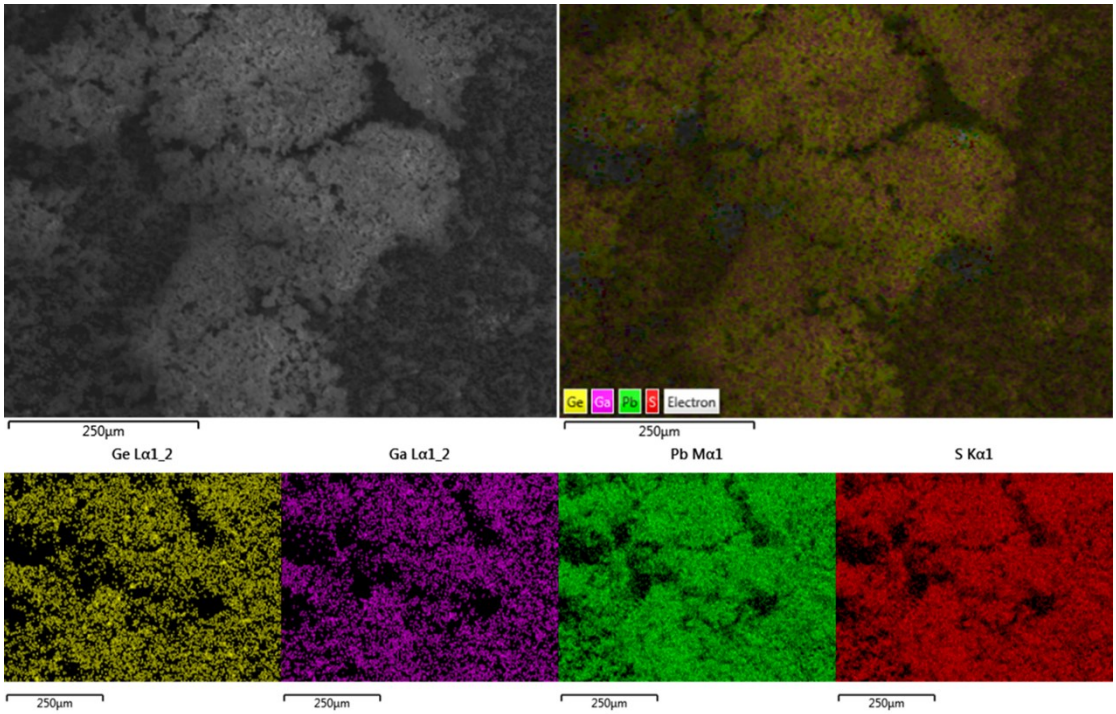

Fig. S3. SEM images and elemental mapping data of Pb^{2+}-loaded material.

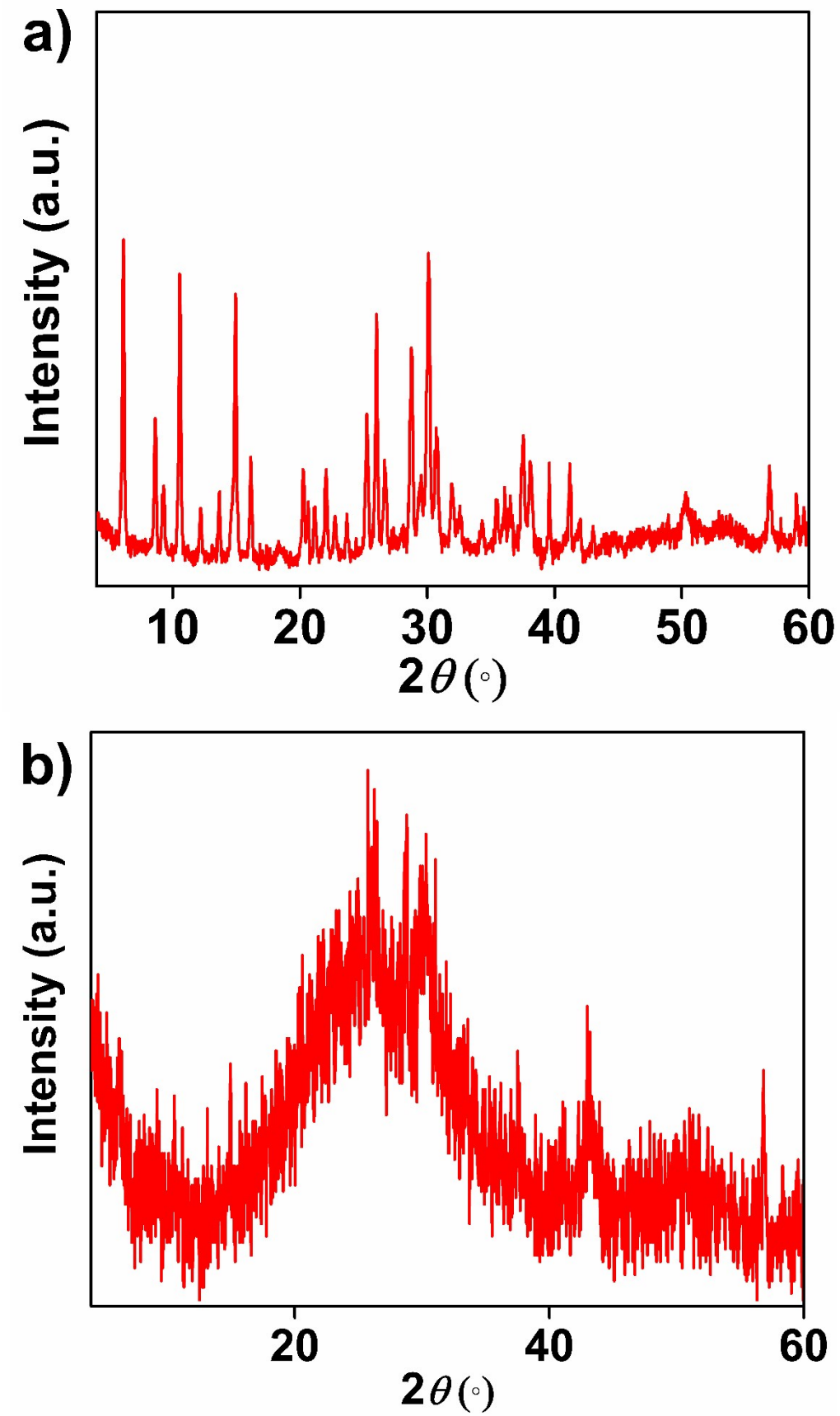

Fig. S4. PXRD patterns **of p-UCR-20** after treatment a) with low Pb^{2+} concentrations (up to 1 ppm) and b) with highly concentrated (1000 ppm) Pb^{2+} solutions.

Table S1. The parameters of Langmuir, Freundlich and Langmuir-Freundlich isotherms, found after the fitting of the isotherm sorption data of Pb^{2+} by the **p-UCR-20**.

	Langmuir			Freundlich			Langmuir -Freundlich			
	q_e (mg/g)	b (L/mg)	R^2	K_F (L/g)	n	R^2	q_e (mg/g)	b (L/mg)	n	R^2
UCR-20	369±26	0.85±0.26	0.94	136±35	6±1.7	0.78	366±30	0.91±0.34	0.92±0.31	0.92
p-UCR-20	621±56	0.02±0.006	0.92	75±27	3±0.6	0.84	527±20	0.03±0.001	0.35±0.06	0.98

Table S2. Comparison of the Pb^{2+} sorption properties of **p-UCR-20** with those of other sorbents.

Sorbent	*Capacity mg/g*	*Equilibrium time*	*Selectivity*	*Reusability*	*ref*
MIL-53(Al) MFC	492.4	120min	-	-	[2]
TMU-5	251	5min	-	-	[3]
Thiol-functionalized $Fe_3O_4@Cu_3(btc)_2$	215.05	120min	vs. various cations	reusable	[4]
MCNC@Zn-BTC	558.66	30min	vs. Cu^{2+}, Zn^{2+}, Cd^{2+}	reusable	[5]
$[Zn_3L_3(BPE)_{1.5}]_n$	616.64	10min	vs. Na^+, Mg^{2+}, K^+, Ca^{2+}, Mn^{2+}, Co^{2+}, Ni^{2+}, Cd^{2+}	reusable	[6]
Ca-MOF	522	5min	vs. Na^+, Mg^{2+}, Ca^{2+}, Ni^{2+}, Zn^{2+}, Cu^{2+}	recyclable	[7]
KMS-1	377	5 min	vs. alkali and alkaline earth cations	Not reusable	[8]
Mg-MTMS	365	120 min	-	reusable	[9]
MoS_4*-LDH*	290	30 min	vs. Co^{2+}, Ni^{2+}, Zn^{2+}, Cd^{2+}	Not reusable	[10]

S_x -LDH	483	-	vs. Zn^{2+}, Co^{2+}, Ni^{2+}	Not reusable	[11]
Duolite GT-73	238	-	-	-	[12]
Amberlite IRC-718	477	-	-	-	[12]
Na^{+}-MOR-1-$NHCS_2$	334	<1min	vs. Na^{+}, Mg^{2+}, Ca^{2+}, K^{+}	recyclable	[13]
p-UCR-20	**527**	**<1min**	**vs. Na^{+}, Mg^{2+}, Ca^{2+}, K^{+}**	**Not reusable**	**This work**

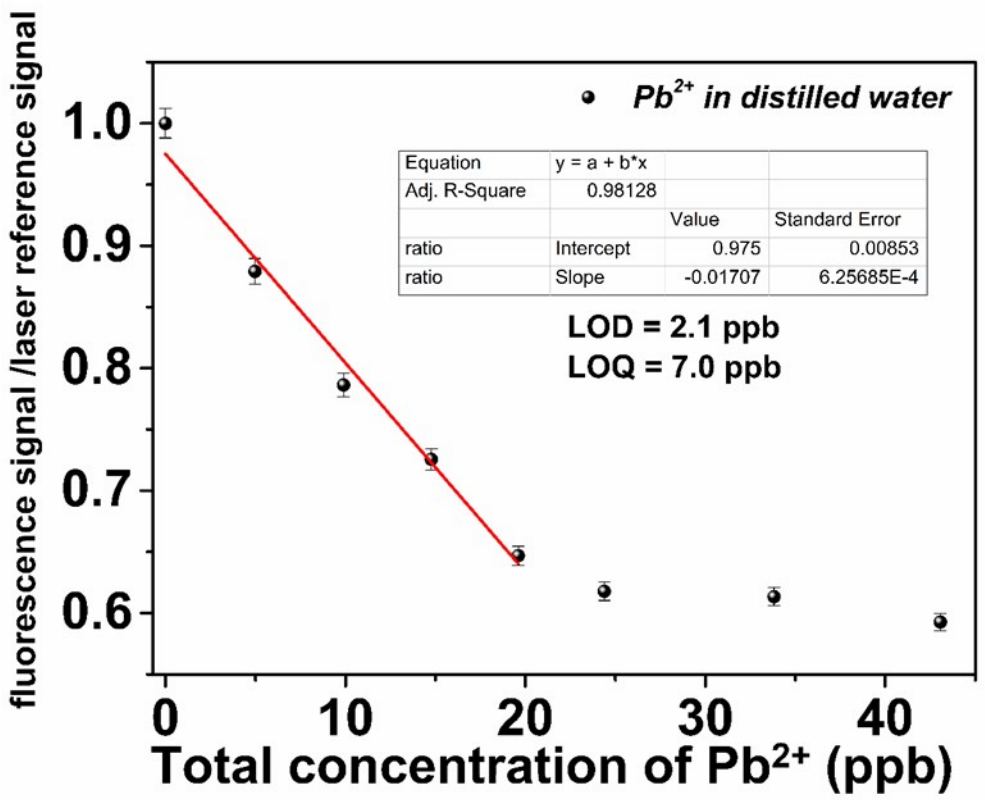

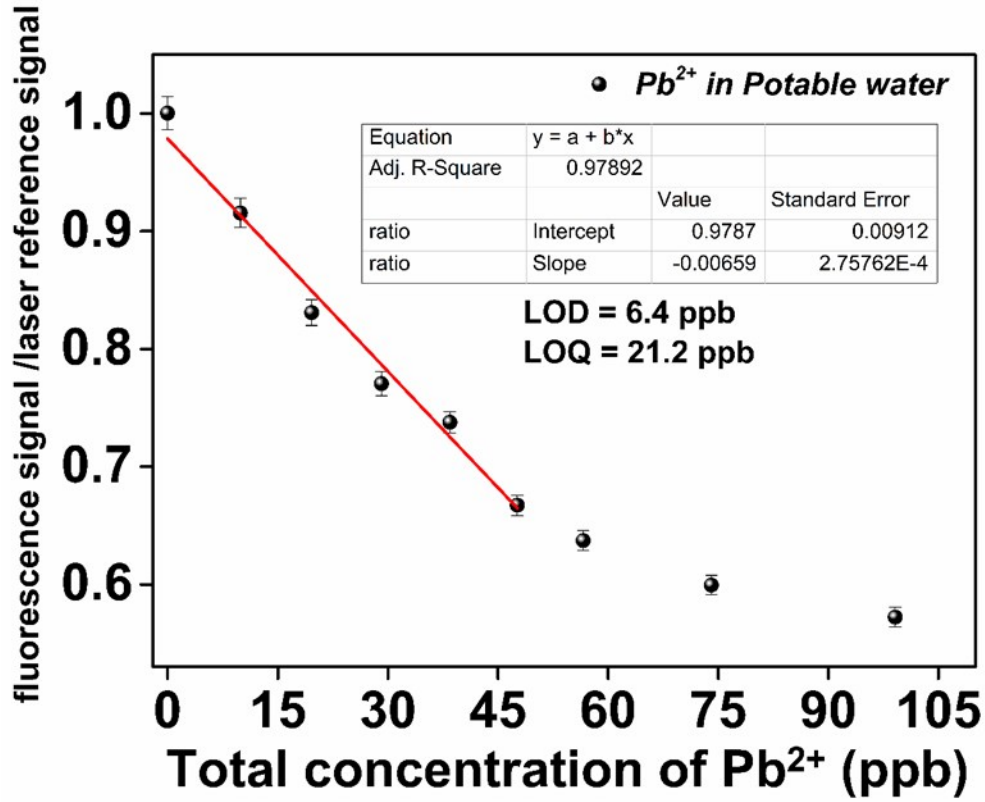

Fig. S5. Calibration curve of the titration of the suspension of **p-UCR-20** in distilled and potable water with Pb^{2+}.

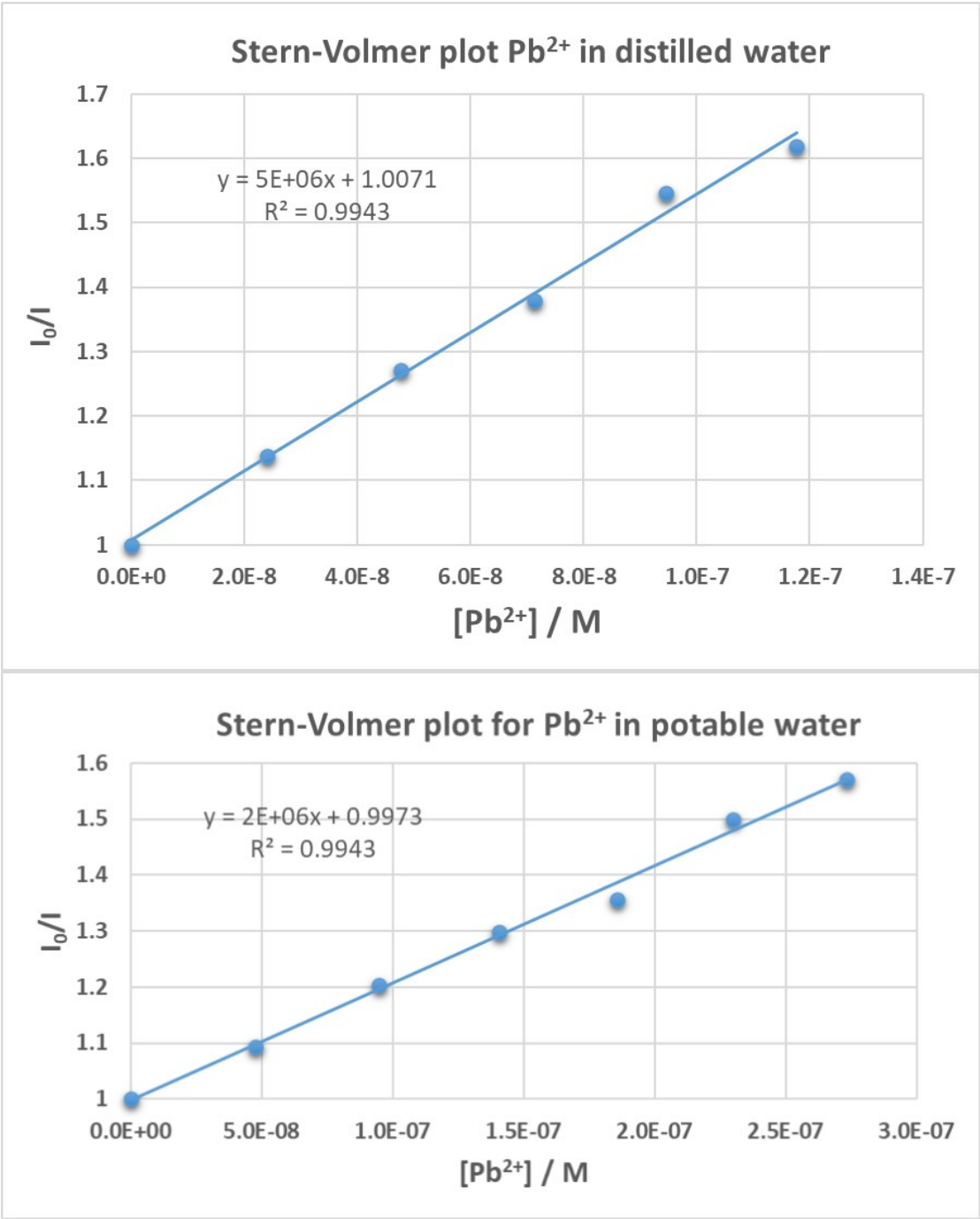

Fig. S6. Stern-Volmer plots for the titration of the suspension of **p-UCR-20** in distilled and potable water with Pb^{2+}.

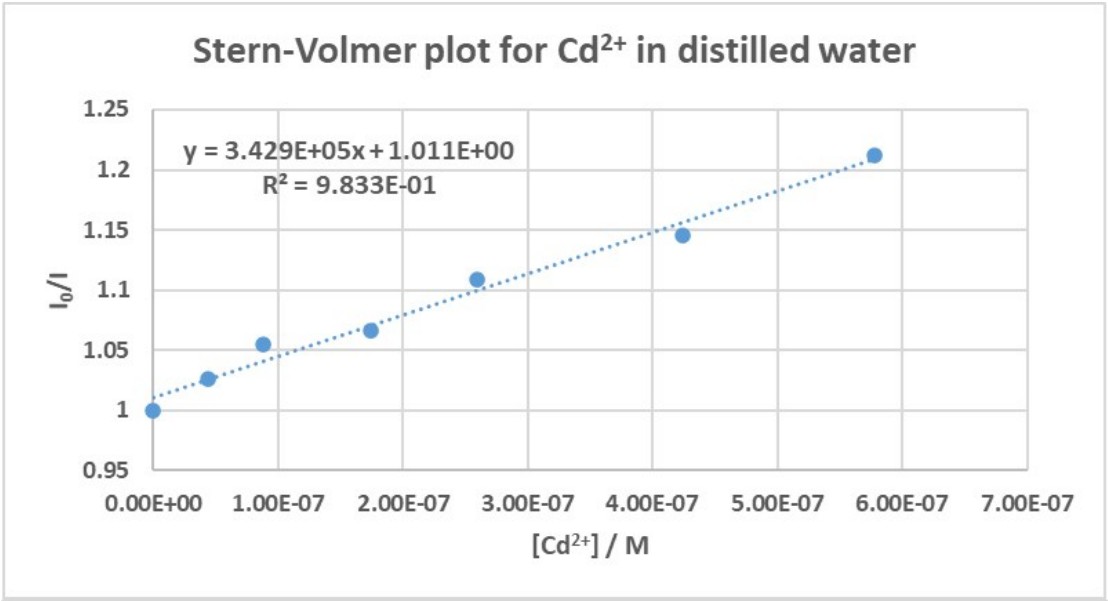

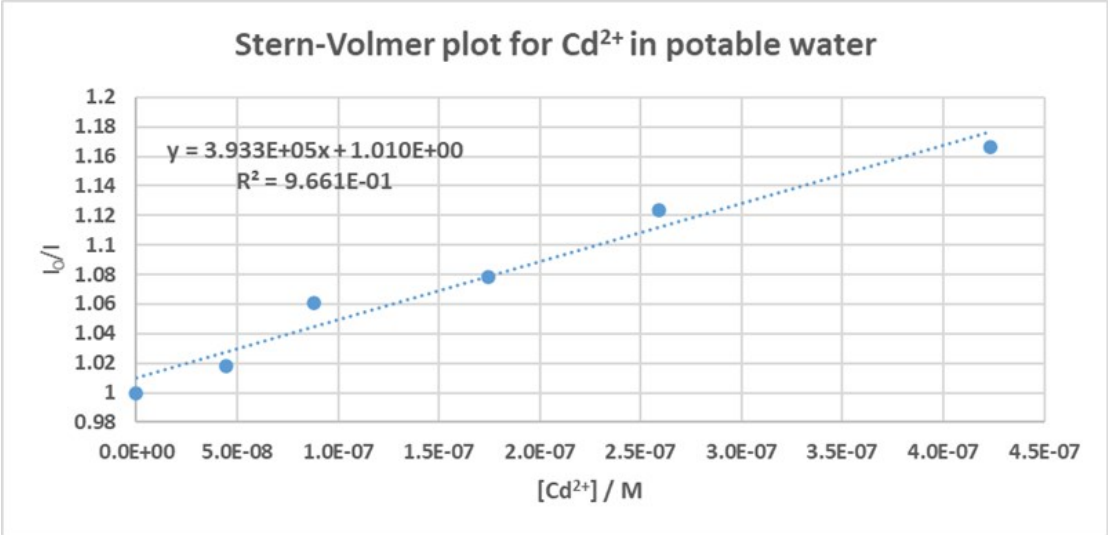

Fig. S7. Stern-Volmer plots for the titration of the suspension of **p-UCR-20** in distilled and potable water with Cd^{2+}.

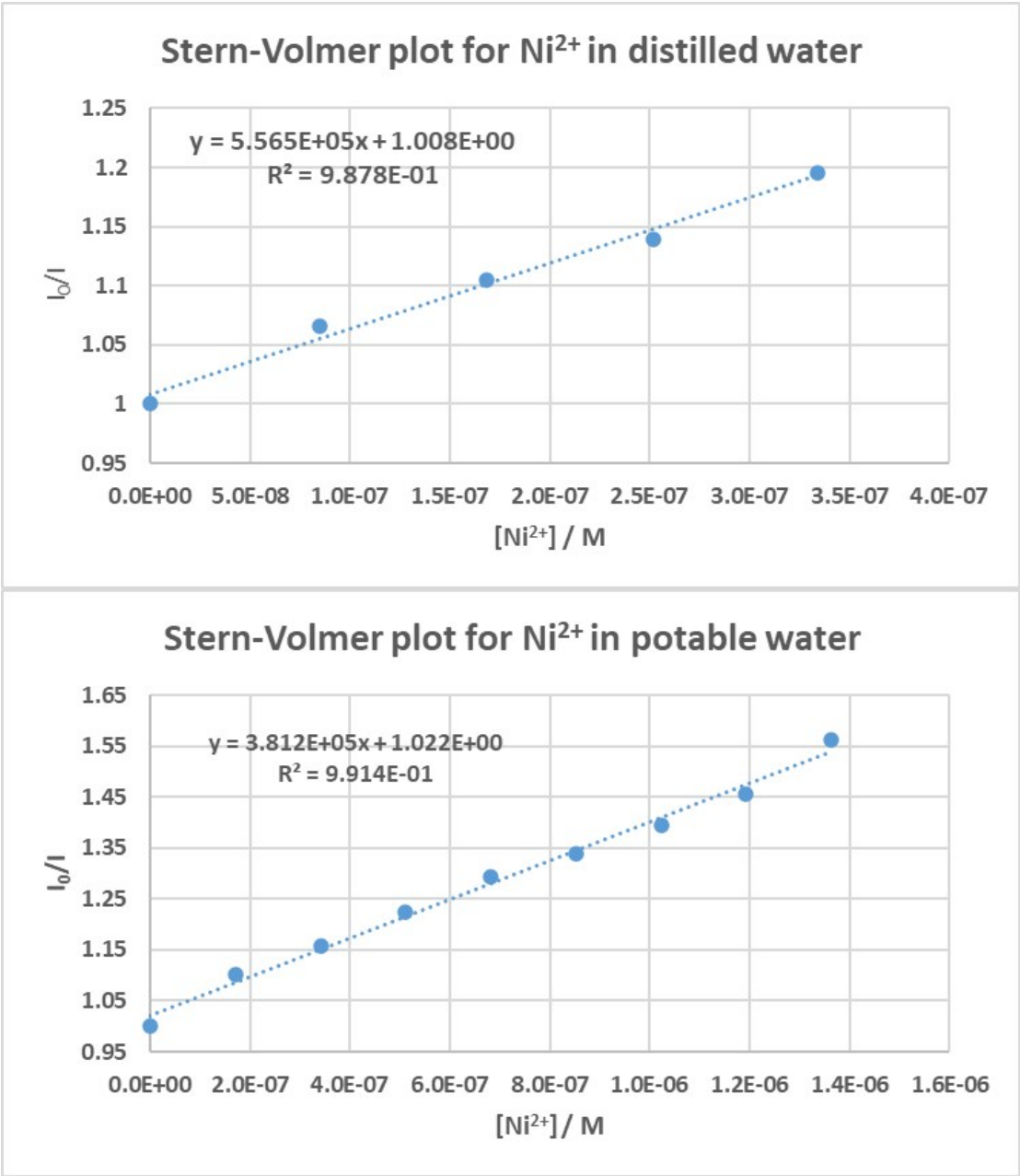

Fig. S8. Stern-Volmer plots for the titration of the suspension of **p-UCR-20** in distilled and potable water with Ni^{2+}.

.

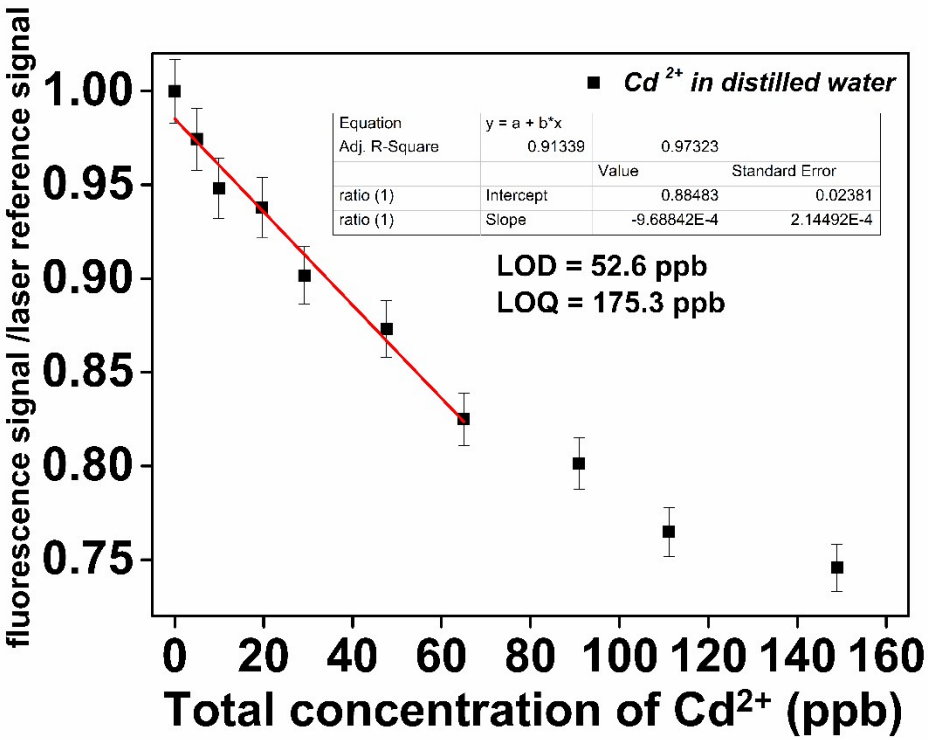

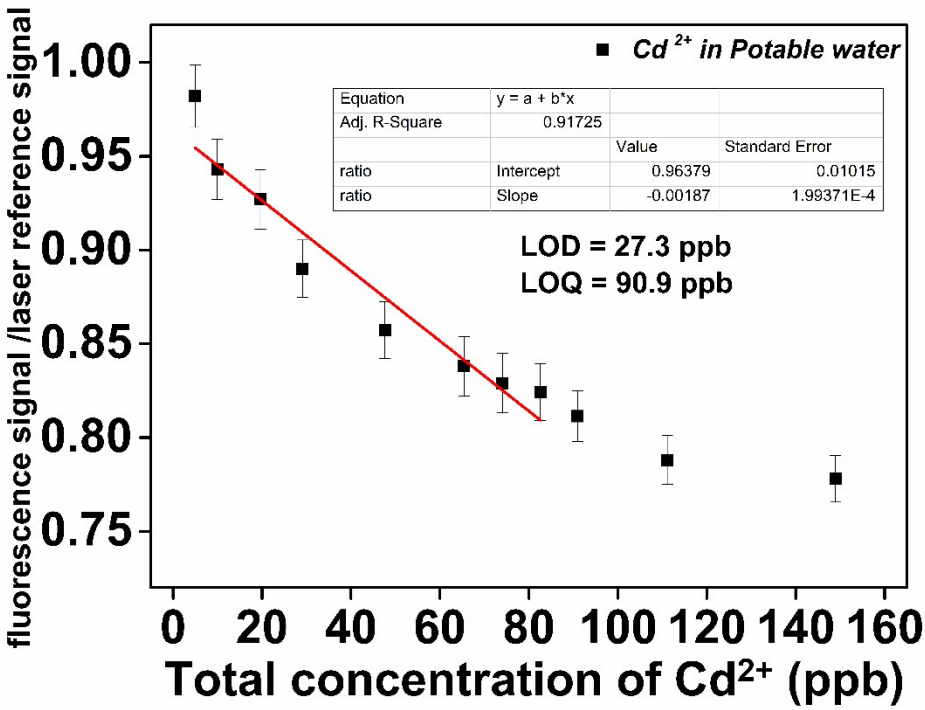

Fig. S9. Calibration curve of the titration of the suspension of **p-UCR-20** in distilled and potable water with Cd^{2+}.

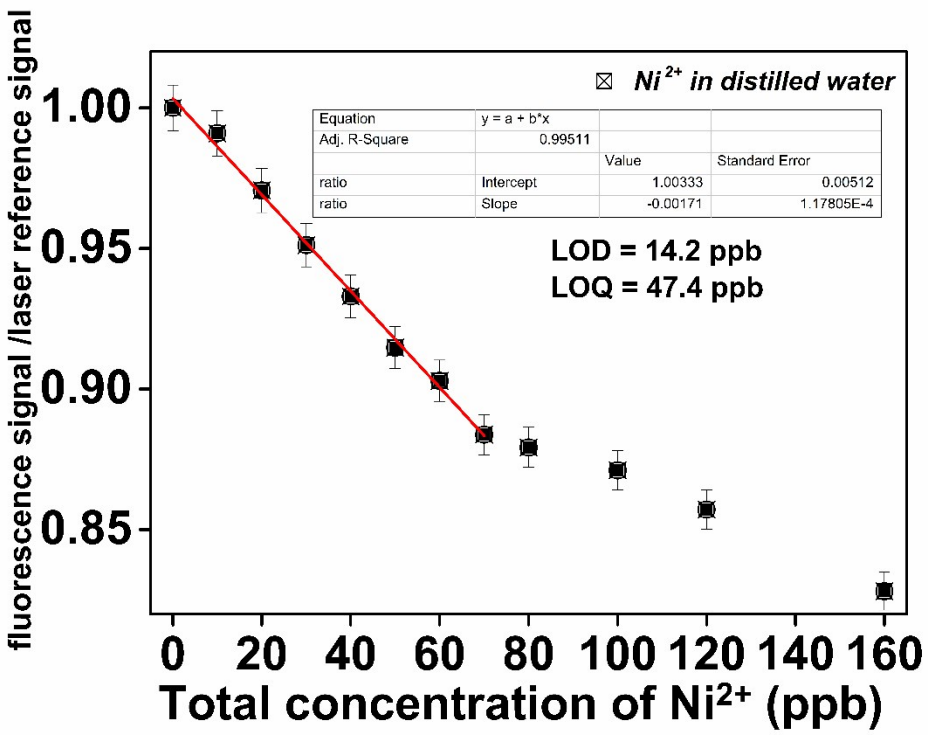

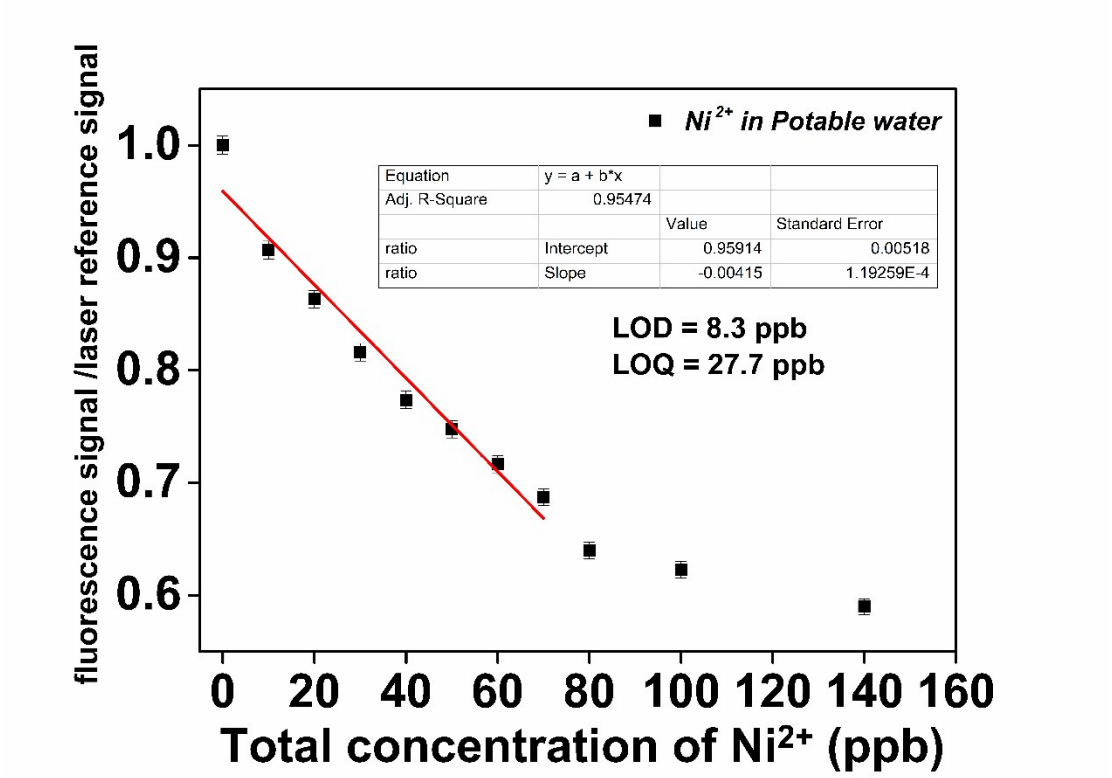

Fig. S10. Calibration curve of the titration of the suspension of **p-UCR-20** in distilled and potable water with Ni^{2+}.

Table S3. Comparative fluorescence quenching data for **p-UCR-20** suspended in distilled and potable water with various metal ions.

Metal ion	Maximum quenching / %	K_{sv} / $10^6 M^{-1}$	LOD / ppb	LOQ / ppb
[a]Pb^{2+}	40	5.3	2.1	7.0
[b]Pb^{2+}	40	2.0	6.4	21.2
[a]Cd^{2+}	25	0.3	52.6	175.3
[b]Cd^{2+}	20	0.3	27.3	90.9
[a]Ni^{2+}	20	0.6	14.2	47.4
[b]Ni^{2+}	40	0.4	8.3	27.7

[a] Distilled water; [b] Potable water

References

1 M. A. Marangoni, D. Brida, M. Quintavalle, G. Cirmi, F. M. Pigozzo, C. Manzoni, F. Baronio, A. D. Capobianco and G. Cerullo, Narrow-bandwidth picosecond pulses by spectral compression of femtosecond pulses in second-order nonlinear crystals, *Opt. Express*, 2007, **15**, 8884.

2 R. Ricco, K. Konstas, M. J. Styles, J. J. Richardson, R. Babarao, K. Suzuki, P. Scopece and P. Falcaro, Lead(II) uptake by aluminium based magnetic framework composites (MFCs) in water, *J. Mater. Chem. A*, 2015, **3**, 19822–19831.

3 E. Tahmasebi, M. Y. Masoomi, Y. Yamini and A. Morsali, Application of mechanosynthesized azine-decorated zinc(II) metal-organic frameworks for highly efficient removal and extraction of some heavy-metal ions from aqueous samples: A comparative study, *Inorg. Chem.*, 2015, **54**, 425–433.

4 F. Ke, J. Jiang, Y. Li, J. Liang, X. Wan and S. Ko, Highly selective removal of Hg^{2+} and Pb^{2+} by thiol-functionalized Fe_3O_4 @metal-organic framework core-shell magnetic microspheres, *Appl. Surf. Sci.*, 2017, **413**, 266–274.

5 N. Wang, X.-K. Ouyang, L.-Y. Yang and A. M. Omer, Fabrication of a Magnetic Cellulose Nanocrystal/Metal–Organic Framework Composite for Removal of Pb(II) from Water, *ACS Sustain. Chem. Eng.*, 2017, **5**, 10447–10458.

6 C. Yu, X. Han, Z. Shao, L. Liu and H. Hou, High Efficiency and Fast Removal of Trace Pb(II) from Aqueous Solution by Carbomethoxy-Functionalized Metal–Organic Framework, *Cryst. Growth Des.*, 2018, **18**, 1474–1482.

7 A. D. Pournara, A. Margariti, G. D. Tarlas, A. Kourtelaris, V. Petkov, C. Kokkinos, A.

Economou, G. S. Papaefstathiou and M. J. Manos, A Ca^{2+} MOF combining highly efficient sorption and capability for voltammetric determination of heavy metal ions in aqueous media, *J. Mater. Chem. A*, 2019, **7**, 15432-15443.

8 M. J. Manos and M. G. Kanatzidis, Sequestration of heavy metals from water with layered metal sulfides, *Chem. - A Eur. J.*, 2009, **15**, 4779–4784.

9 I. L. Lagadic, M. K. Mitchell and B. D. Payne, Highly effective adsorption of heavy metal ions by a thiol-functionalized magnesium phyllosilicate clay, *Environ. Sci. Technol.*, 2001, **35**, 984-990.

10 L. Ma, Q. Wang, S. M. Islam, Y. Liu, S. Ma and M. G. Kanatzidis, Highly Selective and Efficient Removal of Heavy Metals by Layered Double Hydroxide Intercalated with the MoS_4^{2-} Ion, *J. Am. Chem. Soc.*, 2016, **138**, 2858–2866.

11 S. Ma, Q. Chen, H. Li, P. Wang, S. M. Islam, Q. Gu, X. Yang and M. G. Kanatzidis, Highly selective and efficient heavy metal capture with polysulfide intercalated layered double hydroxides, *J. Mater. Chem. A*, 2014, **2**, 10280–10289.

12 S. Chamarthy, C. W. Seo and W. E. Marshall, Adsorption of selected toxic metals by modified peanut shells, *J. Chem. Technol. Biotechnol.*, 2001, **76**, 593–597.

13 A. D. Pournara, S. Rapti, T. Lazarides and M. J. Manos, A dithiocarbamate-functionalized Zr^{4+} MOF with exceptional capability for sorption of Pb^{2+} in aqueous media, *J. Environ. Chem. Eng.*, 2021, **9**, 105474.